Veterinary Microbiology 235 (2019) 220–228

Contents lists available at ScienceDirect

Veterinary Microbiology

journal homepage: www.elsevier.com/locate/vetmic

Application of RNAscope technology to studying the infection dynamics of a Chinese porcine epidemic diarrhea virus variant strain BJ2011C in neonatal piglets

Yueqi Cai, Di Wang, Lei Zhou, Xinna Ge, Xin Guo, Jun Han*, Hanchun Yang

Key Laboratory of Animal Epidemiology of the Ministry of Agriculture, College of Veterinary Medicine, China Agricultural University, Beijing 100193, People's Republic of China

ARTICLE INFO

Keywords:
PEDV
Neonatal piglets
Infection dynamics
Infection characteristics
RNAscope

ABSTRACT

The highly virulent porcine epidemic diarrhea virus (PEDV) variants cause the death of mainly neonatal piglets, but how the viruses spread within the gastro-intestinal tract in a temporal and spatial manner has remained poorly characterized but is critical to understand the viral pathogenesis. In this study, we used the Chinese PEDV epidemic strain BJ2011C as a model organism and took advantage of the newly developed RNAscope in situ hybridization technology to investigate the tempo-spatial infection dynamics in neonatal piglets. We found that the PEDV strain BJ2011C could quickly colonize the small intestine, which occurred in just 6 h post infection, with virus shedding starting at 6 hpi and peaking at 24 hpi. Jejunum was the first target tissue for infection and then ileum, followed by infrequent infection of duodenum. In these tissues, the virus nucleic acids were mainly present in the villous epithelial cells but not in crypt cells. Interestingly, the viral RNAs were not detectable by RNAscope in large intestines although tissue damages could be discerned by H & E staining. Overall, our results provide useful information about spread dynamics and tissue preference of PEDV epidemic strain BJ2011C.

1. Introduction

Porcine epidemic diarrhea virus (PEDV) is the etiological agent of porcine epidemic diarrhea (PED), a highly contagious swine enteric disease that is manifested as acute diarrhea, vomiting and dehydration in the field (Song and Park, 2012; Stevenson et al., 2013b; Sueyoshi et al., 1995). This microbe was first identified in 1978 by a group of scientists from Europe and phylogenetically belongs to the genus *Alphacoronavirus* within the family *Coronaviridae* in the order *Nidovirales* (Pensaert and Debouck, 1978). Due to the vaccination intervention, PEDV generally caused sporadic and endemic epidemics in the past with a relatively low impact despite its prevalence in many swine producing countries such as those in European and Asia (Choudhury et al., 2016; Hur, 1993; Sun et al., 2015; Takahashi et al., 1983; Wang et al., 2016). The great turning point is the year late 2010 when a highly virulent PEDV variant emerged in a mysterious manner in Chinese swine farms and caused fatal consequences to neonatal piglets of less than one-week old (Al, 2012; Min et al., 2015; Sun et al., 2012; Xiao-Meng et al., 2013). Three years later, PEDV variants descended on the land of North America and spread rapidly nationwide in the United States and also to other countries, leading to the death of millions of pigs (Changhee, 2015; Elena et al., 2016; Stevenson et al., 2013a; Vlasova et al., 2014). As of today, the PEDV novel variants have remained a big concern to the major swine-producing countries worldwide.

The pathogenicity of several highly virulent strains has been studied in the model of neonatal piglets. Virus-induced damages are mainly localized to Jejunum and Ileum, but lesions can also be found in other segments of large intestine (Jung et al., 2015a; Lin et al., 2015b; Stevenson et al., 2013a). However, the PEDV novel variants appear to vary in tissue distribution. For some viruses (e.g. PC21A, US/Iowa/18984/2013, PC22A, etc.), virus antigen or RNA can be detected in colon, but some (USA/KS/2013) are not (Jung et al., 2015a, 2014; Lin et al., 2017; Madson et al., 2014). Moreover, the virus detection in these studies is mainly based on assays such as PCR and immunohistochemistry staining (IHC) with specific antibodies or DNA probes. The PCR-based assay is highly sensitive, but the tissues can be potentially contaminated by intestinal contents. The challenge for IHC is the high level of nonspecific tissue staining although the antibodies to PEDV generally work well in cell culture. Traditional in situ RNA

* Corresponding author at: Department of Preventive Veterinary Medicine, China Agricultural University College of Veterinary Medicine, 2 Yuanmingyuan West Road, Haidian District, Beijing 100193, People's Republic of China.
E-mail address: hanx0158@cau.edu.cn (J. Han).

https://doi.org/10.1016/j.vetmic.2019.07.003
Received 26 March 2019; Received in revised form 29 June 2019; Accepted 6 July 2019

Table 1
Experimental design for animal studies.

Group	n	Age (days)	Inoculation#	Pigs euthanized or died at given hours post inoculation						
				6	12	24	48	72	84	96
Control	2	2	DMEM							all
A	6	2	PEDV (1×10^5 PFU/mL)	A1	A2	A3	A4	A6#		A5#
B	6	2	PEDV (1×10^5 PFU/mL)	B1	B2	B3	B4		B5#, B6#*	

Inoculation via oro-grastric catheter; dose: 5 mL; #: Piglets died of PED.

detection techniques (ISH and FISH) have been around for years, however, they generally lack robustness and sensitivity to reliably detect the gene expression (Jensen, 2014). Considering the potential caveats, it is necessary to require a more sensitive and robust method to further characterize the tissue distribution in situ of PEDV variants. With such a method available, it will also be helpful to understand spread dynamics of virulent PEDV variants within the gastro-intestinal tract in a temporal and spatial manner, the knowledge of which is currently lacking but critical to understand the viral pathogenesis.

RNAscope is a newly developed RNA ISH technology with a unique probe design strategy that allows simultaneous signal amplification and background suppression to achieve single-molecule visualization while preserving tissue morphology (Wang et al., 2012). It can use either conventional chromogenic dyes for bright-field microscopy or fluorescent dyes for multiplex analysis. In this study, we used the Chinese PEDV epidemic strain BJ2011C as the model organism and applied this technology in conjunction with other methods to characterizing the infection dynamics in neonatal piglets (Li et al., 2017). Our results showed that PEDV strain BJ2011C could quickly colonize the small intestine in 6 h post infection (hpi). Jejunum is the first infected tissue before viral spread to ileum, followed by infrequent infection of duodenum. In these tissues, the viral nucleic acids were mainly present in the villous epithelial cells. Interestingly, RNAscope did not detect viral RNA in large intestines although tissue damages could be discerned by H&E staining. Our results provide useful information about PEDV spread and tissue preference.

2. Materials and methods

2.1. Ethics statement

The animal experiments were performed according to the Chinese Regulations of Laboratory Animals The Guidelines for the Care of Laboratory Animals (Ministry of Science and Technology of People's Republic of China) and Laboratory Animal-Requirements of Environment and Housing Facilities (GB 14925 ± 2010, National Laboratory Animal Standardization Technical Committee). The license number associated with this research protocol was CAU20180121-2, which was approved by the Laboratory Animal Ethical Committee of China Agricultural University.

2.2. Virus and cells

The isolation of PEDV strain BJ2011C used in this study were reported previously by our laboratory (Li et al., 2017). It was isolated on Vero CCL-81 cells from small intestine samples of pigs with PED symptoms. Vero CCL-81 cells were maintained in Gibco Dulbecco's modified Eagle medium (DMEM) containing 10% fetal bovine serum at 37 °C with 5% CO_2. The propagation of PEDV BJ2011C requires supplementation of trypsin at 10 μg/mL as previously described (Hofmann and Wyler, 1988).

2.3. Animal experiment design

Fourteen 2-day-old piglets were randomly divided into control (n = 2) and challenged (n = 12) groups. The challenged group was subdivided into 2 groups (A and B) with 6 piglets for each group. Pigs in A and B group were numbered from No.1 to 6. Groups A, B and control were housed in each isolator. The piglets were fed with a mixture of bovine colostrum powder and fresh liquid milk every four hours. Before challenge, the piglets were confirmed negative for PEDV (Wang et al., 2018), TGEV (Kim et al., 2000), PDCoV (Jung et al., 2015b), Rota virus (Amimo et al., 2013a, b) by using PCR. After 1 day for adaptation to the environment, the pigs were orally inoculated with 5 mL dose of 1×10^5 plaque-forming unit (PFU)/mL. The control group was mock-infected with 5 mL DMEM. Every two piglets were randomly selected for necropsy at 6, 12, 24 and 48 h post-inoculation (hpi). One or two piglets were euthanized at 72, 84 and 96 hpi according to their symptoms. And piglets in control group were euthanized at 96 hpi (Table 1). Fecal swabs were collected at 6, 12, 24, 48, 72, 84 and 96 hpi from all remaining pigs (Table 1).

2.4. Clinical assessment

The animals were monitored every 8 h for clinical signs of disease. The total number of pigs with clinical diarrhea were subjectively scored for fecal consistency using the following criteria as described previously (Li et al., 2017; Wang et al., 2018): 0, normal; 1, soft; 2, very soft and tend to be liquid; 3, liquid with some solid content; 4, watery diarrhea with no solid content, respectively. Fecal scores were recorded daily until they were euthanized.

2.5. Gross and histopathological examination

At necropsy, gastrointestinal tissues were examined. Fresh and formalin fixed sample collections include stomach, duodenum, mid-jejunum, mid-ileum, cecum, mid-colon and rectum. After 48 h fixation in 10% neutral buffered formalin, tissue sections were trimmed, dehydrated in graded alcohol, and embedded in paraffin. Micro sections were cut and stained with hematoxylin and eosin (H & E) (Li, et al., 2017).

2.6. RNA in situ hybridization

The RNAscope in situ hybridization (ISH) method for formalin-fixed paraffin-embedded (FFPE) tissues has been previously described (Wang et al., 2012). To detect the distribution of PEDV nucleic acids in intestinal tracts, in situ hybridization (ISH) in formalin-fixed, paraffin-embedded (FFPE) intestinal tissues was performed using the RNAscope® Multiplex Fluorescent Reagent Kit v2 (Cat. No. 323100, Advanced Cell Diagnostics, lnc., USA) according to the manufacturer's instructions. Briefly, 20 double Z probe pairs specifically targeting the region coding for PEDV nucleocapsid protein were designed and synthesized by ACD. Each probe forms a 28-base hybridization with the targeted RNA for the preamplifier containing 20 binding sites for the amplifier. Probes were fluorescently labeled with cyanine 3 for direct visualization under a fluorescence microscope. For tissue processing, the formalin-fixed paraffin-embedded (FFPE) intestinal tissues were cut into 5-μm thickness, and tissue sections on slides were baked in a dry oven at 60 °C for 1 h before being deparaffinized in xylene and

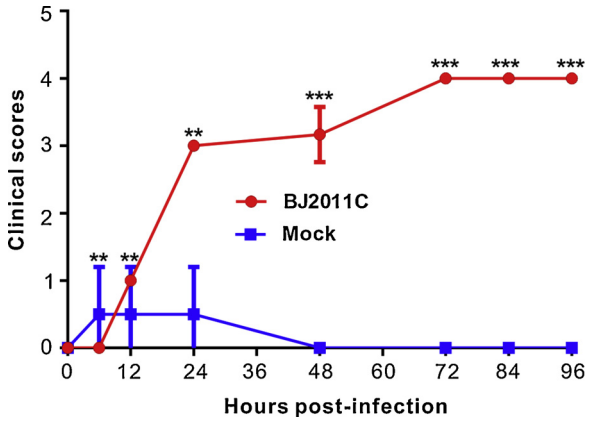

Fig. 1. Fecal scores of piglets at different hours post inoculation. After inoculation, piglets were monitored for clinical signs at given time. Fecal scores were used to assess diarrhea. Evaluation standard: 0 = normal; 1 = soft (cowpie); 2 = very soft and tend to be liquid; 3 = liquid with some solid content; 4 = watery diarrhea with no solid content. Asterisk (*) indicates a significant difference between control and challenged group (**P < 0.01; ***P < 0.001).

dehydrated in ethanol series. Finally, placing slides on absorbent paper with the section face-up and air-dry slides for 5 min at RT. Following that, the sections were treated with several drops of RNAscope Hydrogen Peroxide for 10 min at RT and then washed in distilled water for 3–5 times. Afterwards, tissue sections were incubated in citrate buffer (10 nmol/L, pH 6) maintained at a boiling temperature for 15 min. Immediately, tissue sections were rinsed in deionized water and transferred into 100% alcohol for 3 min and drying slides in 60 °C incubator. Next, tissue sections were treated with 10 μg/ mL protease at 40°C for 30 min in a HybEZ hybridization oven (ACD) and washed 3–5 times in distilled water. Then, tissue sections were incubated in order at 40°C with following reagents: target probes for 3 h; preamplifier for 30 min; amplifier for 15 min; and label probe for 15 min. For each hybridization step, tissues were rinsed with wash buffer 3 times at RT after treatment. Hybridization signals were detected by TSA® Plus Cyanine 3 (NEL744E001KT, PerkinElmer). At last, the sections on glass slides were counterstained with 4′,6-diamidino-2-phenylindole (DAPI). The images were captured by a Nikon A1 confocal microscope and processed by image J.

2.7. PEDV RT-qPCR

The fecal swabs collected at different times for measuring virus shedding and different sections of intestinal tissues collected from euthanized piglets for quantitation of virus abundance were determined by TaqMan real-time RT-PCR with the primers and probes targeting PEDV N gene as described previously (Li et al., 2017). Briefly, viral RNA was extracted from samples and then 1 μL of each template was used in PCR set-up for a 25 μL total reaction using Quant One Step qRT-PCR kit (TIANGEN Biotech). The sequences of primers and probe (Invitrogen TM) were as follows: Forward primer: 5′-AATCCAGGGCCACTTC GAA-3′; Reverse primer: 5′-TTCGCCCTTGGGAATTCTC-3′; Taqman probe: 5′-AACGTGACCTCAAAGACATCCCAGAGTGG-3′. RT-PCR was carried out using an applied Biosystem 6500 real-time PCR machine as follows: 50°C for 30 min, 92°C for 3 min, and 45 cycles of 92°C for 10 s, 55°C for 20 s and 68°C for 31 s. The standard cure was established as follows: the conserved region (nt 794 to 864) of BJ2011C strain N gene were cloned into pEASY-BLUNT vector (TransGen Biotech) as the PEDV N gene standard plasmid. Then a series of 10-fold dilutions ranging 100 to 10^{-10} ng/μL were prepared as the standard sample to make the standard curve. The threshold was set at 0.05 in result analysis. Based on standard curve, the virus concentration (shown as genomic copy numbers/ mL or g) in those samples was calculated.

2.8. Statistical analyses

The means ± standard error of the mean (SEM) or standard deviation of the means (SDM) was used in expression of all values. Clinical assessment, viral RNA genomic copies in fecal swabs and tissues were analyzed using GraphPad Prism software (GraphPad Prism Inc.).

3. Results

3.1. Clinical assessment

We have previously reported that PEDV epidemic strain BJ2011C belongs to GIIb subtype and is highly virulent to neonatal piglets (Li et al., 2017; Wang et al., 2018). However, how this virus spreads in vivo have remained unclear. To investigate the infection dynamics, 14 two-day-old piglets were randomly divided into 3 groups with 2, 6 and 6 pigs (see Table 1), respectively. The pigs were inoculated orally with BJ2011C at a dose of 5×10^5 PFU or mock-infected with DMEM. All piglets in both control and challenged groups were spirited and showed normal fecal consistency before inoculation. Piglets in mock-infected group were normal during the study, except that they had pasty feces during 6–24 hpi likely because of the stress caused by transport and then returned to normal (Fig. 1). On the other hand, a portion of PEDV-challenged piglets began to display mild diarrhea with soft feces at 12 hpi, and all of them showed semi-solid to watery feces accompanied by lethargy and dehydration at 24 hpi and continued toward end of the study (Fig. 1). And the symptom of diarrhea persisted until death (Fig. 1). Thus, these results confirmed the reported highly virulent feature of BJ2011C, and also suggest that the incubation period was about 12–24 h with the infection of PEDV strain BJ2011C.

3.2. Virus shedding

PEDV RNA in fecal swabs collected from challenged piglets at different times were detected by quantitative Real Time RT-PCR (Fig. 2). Fecal viral RNA can be detected at 6 hpi with a mean genomic copy number/mL of 1.77×10^6 (SEM ± 4.03×10^5) and peaked ($5.66 \times 10^9 \pm 9.74 \times 10^7$ copies/mL) at 24 hpi. The fecal shedding diminished slightly but still kept at a high level thereafter until the end. Thus, the virus shedding started much earlier than the appearance of the clinical symptoms.

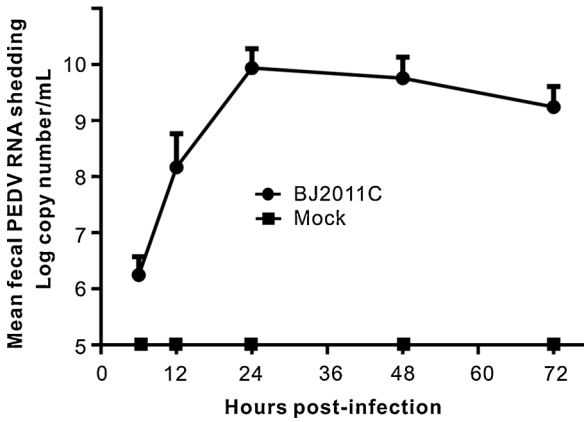

Fig. 2. Virus shedding in feces. Fecal swabs were collected at 6, 12, 24, 48 and 72 hpi after inoculation. Virus shedding at different hours post inoculation was measured by Real-Time RT-PCR detection of virus genome in fecal swabs using the TaqMan probe targeting PEDV N gene. The length of target fragment is 618 bp.

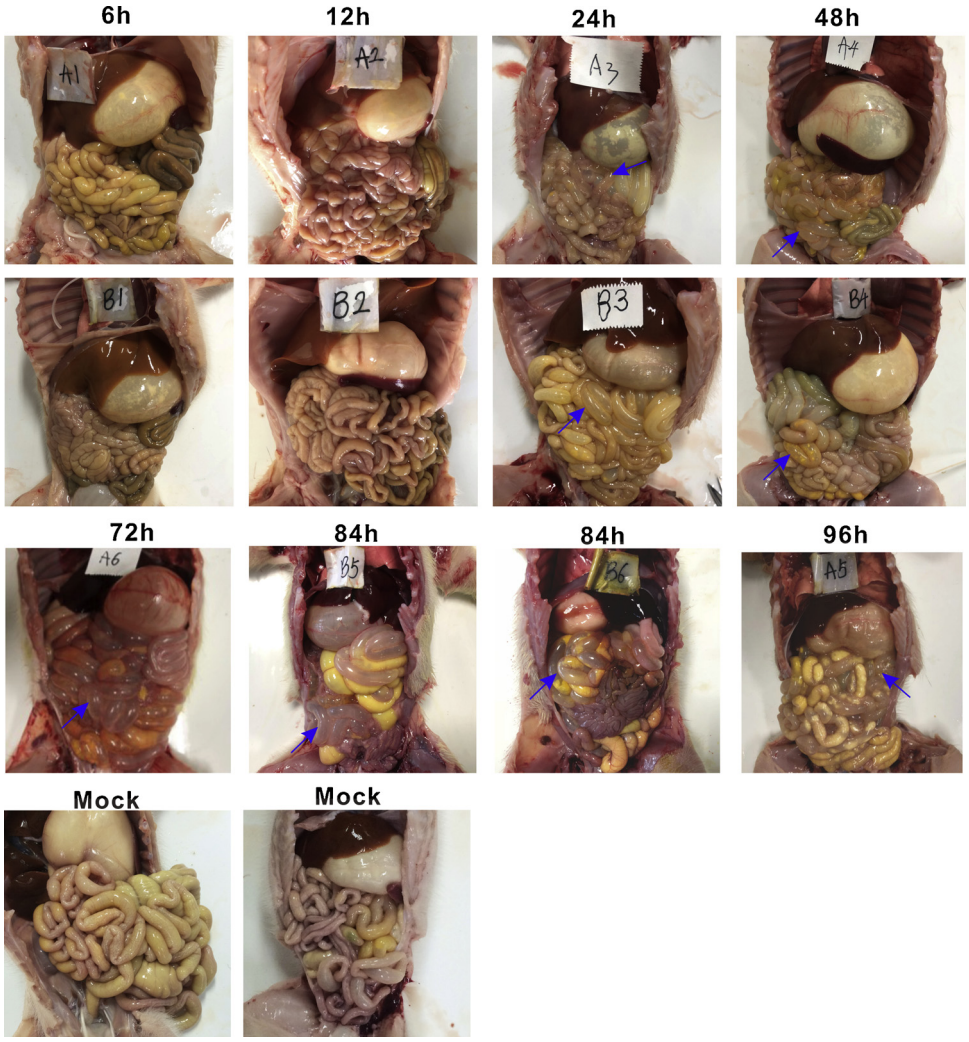

Fig. 3. Gross lesions of piglets inoculated with BJ2011C at different hours post inoculation. The intestinal lesions were examined at the given hours of death or euthanasia at different hours post inoculation. Piglets in control group were euthanized at 96 hpi in the end. Necropsy images showed that transparent intestines with yellow fluid contents (arrowheads) were observed in infected piglets from 24 to 96 h post-inoculation but not in mock-inoculated piglets.

3.3. Gross lesions

By gross observation, there were no evident lesions that could be observed in inoculated piglets at 6 and 12 hpi except that one piglet numbered as A1 showed accumulation of large amounts of yellowish fluid in small intestinal lumen. All inoculated piglets began to exhibited generally transparent intestinal walls, yellowish fluid in intestinal lumens and the stomachs were filled with curdled milk at 24 hpi, a time point that was consistent with the result of clinical assessment. The gross lesion became more obvious as the infection proceeded. But one piglet numbered as A6 euthanized at 96 hpi showed mild lesions compared with piglets euthanized at 72 or 84 hpi. On the other hand, no evident gross lesions were found in negative controls (Fig. 3).

3.4. Histologic lesions

By microscopic examination, no obvious lesions were found in stomach, caecum, colon and rectum of all challenged piglets at any time (Fig. 4). There were no histologic lesions evident for all gastrointestinal tissues of inoculated piglets euthanized at 6, 12 and 24 hpi. Mild blunting, fusion and atrophy villi were observed only in jejunum and ileum of piglets euthanized at 48 hpi. The most severely and extensively scattered, disrupt and fusion villi of all small intestine including duodenum, jejunum and ileum in piglets euthanized at 72 and 84 hpi. The piglet euthanized at 96 hpi mainly had severe blunting and fusion villi in small intestine. No significant gross lesions were noted in the control piglets.

3.5. Viral tissue load

The viral RNAs in the different gastrointestinal tissues at different hpi were quantified by qRT-PCR targeting N protein-coding region (Fig. S1). PEDV RNAs could be were detected at 6 hpi in all tissues with the highest viral load in jejunum. The first peak of viral load appeared at 24 hpi in all tissues except for the jejunum, perhaps due to the cellular damage. Afterwards, the RNA load in stomach, duodenum, ileum, colon and rectum continued to decline until 72 hpi, a point when the viral load increased again for unclear reasons. Overall, the viral load in the stomach fluctuated slightly, and jejunum and ileum maintained relatively higher viral load than other tissues, suggesting that they are the major targets of PEDV infections.

3.6. Dynamics of viral infection and spread by RNA scope

RNAscope, a new technology for in situ RNA hybridization, was used to detecting PEDV nucleic acids in situ in tissues of piglets. Positive signals were firstly and only detected in the jejunum villi of one inoculated piglet but not for the jejunum of the other piglet euthanized

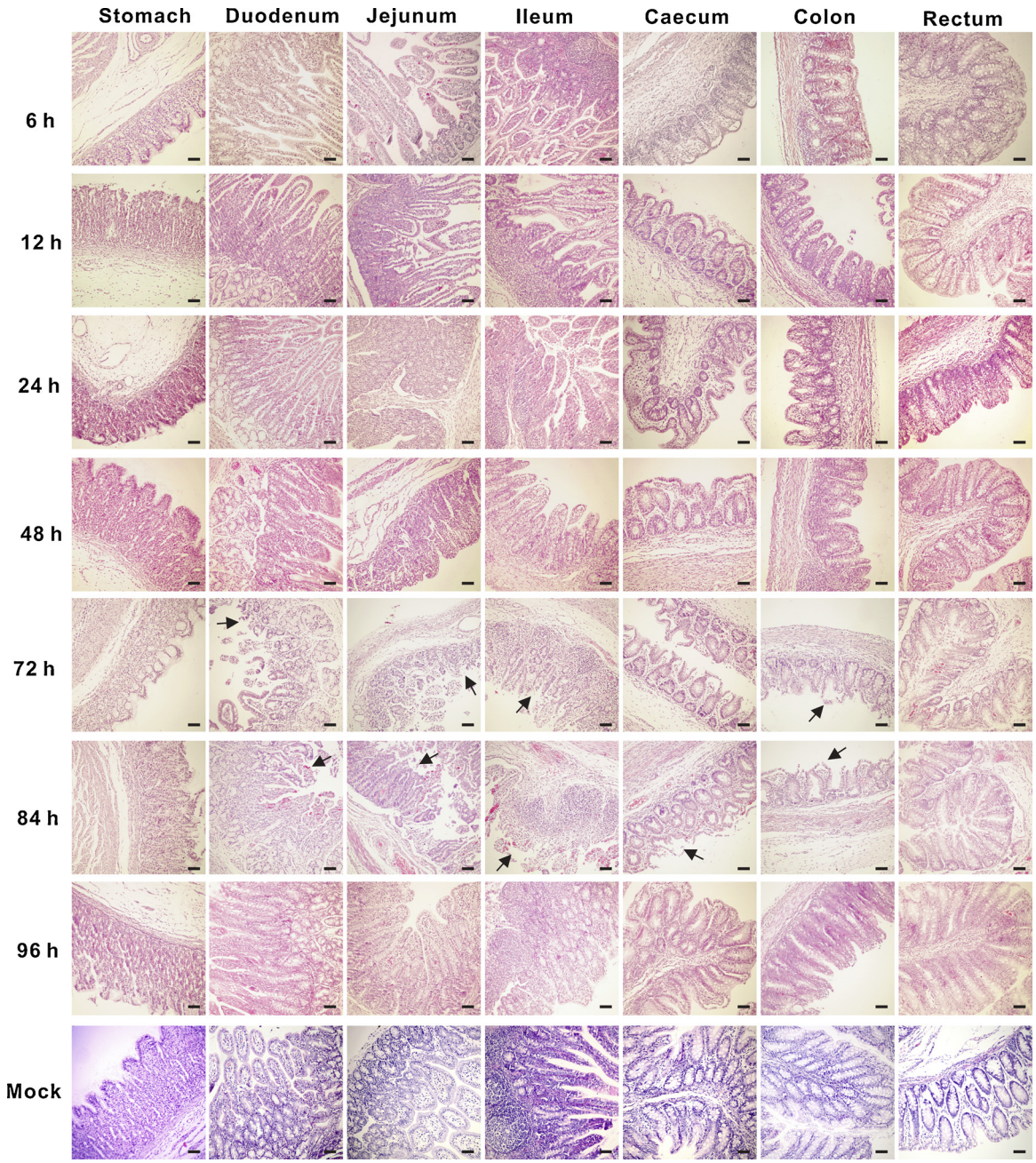

Fig. 4. Histopathological examination of stomach and intestines of BJ2011C-infected piglets. At different hours post inoculation, different segments including stomach, duodenum, jejunum, ileum, caecum, colon and rectum from piglets were taken after euthanasia and then processed for HE staining. Piglets from 48 to 96 hpi showing intestinal villous epithelial injury including blunting, fusion and astropy villi and vacuolation (arrowheads) in different degrees. Bar = 500 μm.

at 6 hpi. At 12 hpi, positive signals became stronger in the jejunum of piglets. Apart from the signals in jejunums, weaker signals were also found in the villi of ileum in one piglet euthanatized. After 12 hpi, all challenged piglets were ISH positive in the jejunum and ileum (Fig. 5), but signals in the ileum became stronger than that in jejunum. In general, the positive epithelial cells were arranged continuously in the villous enterocytes of the small intestine (Fig. 6). Notably, there were a few hybridization signals in the villi of duodenum in one piglet euthanatized at 96 hpi. And this is the only piglet which was positive in the duodenum. None of the twelve piglets in challenged group was ISH positive in the caecum, colon or rectum and PEDV RNA were not detected in any tissue from the piglets in control group. Thus, jejunum and ileum are the major targets of PEDV BJ2011C, and the infection progresses in an orderly manner. That is, the virus first infects jejunum and spreads to the ileum, followed by duodenum.

For retrospective analysis, we also performed the RNAscope in situ hybridization assay of our previous studies samples (Wang et al., 2018) (Fig. S2). The results were similar to this study. That is, the viral nucleic acids of BJ2011C were present in situ only in small intestine, but NOT detectable in large intestine. As the negative control, we could not detect CHM2013 RNAs in any intestinal tissues. In the gain of function test, when the CHM2013 structural protein-coding region (SP) was replaced by the BJ2011C SP (CHM2013-$SP_{BJ2011C}$), the CHM2013 RNA could be detected by RNAcope. In the loss of function assay, when the SP region of BJ2011C is replaced by the corresponding region of CHM2013 (BJ2011C-$SP_{CHM2013}$), RNAscope failed to detect viral nucleic acids of BJ2011C in situ. Thus, these results are consistent with our overall conclusions in that paper and also the findings here.

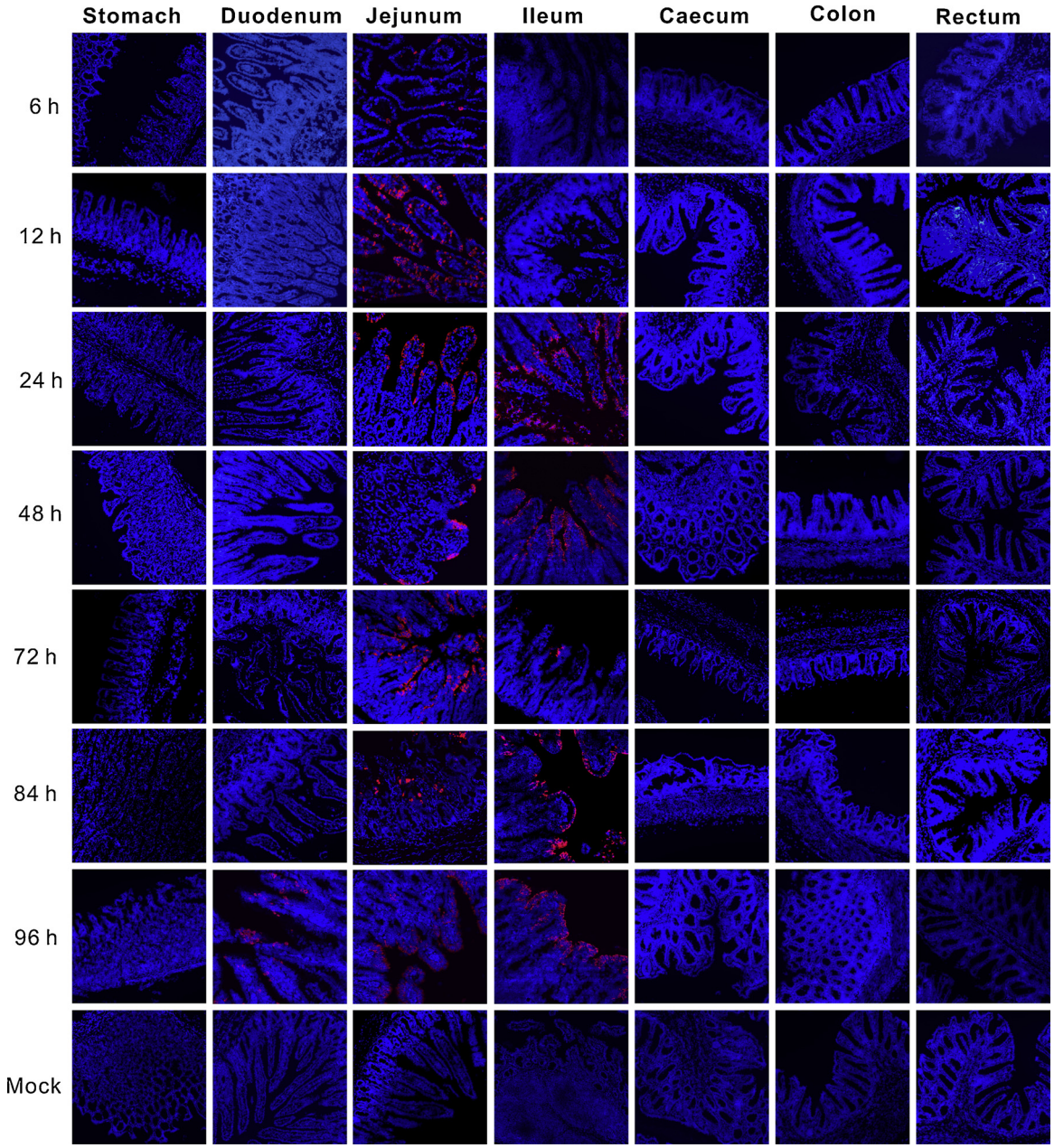

Fig. 5. Viral RNA distribution by ISH in different tissues. PEDV RNA were detected by RNA in situ hybridization in different tissues of experimentally infected neonatal piglets euthanatized at different hours post inoculation and mock-infected piglets euthanatized at 96 hpi. Tissues were stained with PEDV-N target probe (red). Cell nuclei were counterstained with DAPI (blue). Original magnification, ×200.

4. Discussion

PEDV variants have been prevalent in China since 2010, causing serious losses to the swine industry (Al, 2012; Rui-Qin et al., 2012; Xiao-Meng et al., 2013). They can infect piglets of all ages, but the highest mortality occurs to suckling piglets within 1 week old (Rui-Qin et al., 2012; Shibata et al., 2000). Thus, it is of critical importance to understand the infection dynamics in neonatal piglets of PEDV epidemic strains for developing better strategies for the disease prevention and control. By using the BJ2011C from G2b subtype as the model organism and 2-day-old piglets as animal model, we revealed the following important information following natural route infection. i) PEDV strain BJ2011C can quickly colonize small intestine as early as 6 hpi; ii) the disease had a quite short incubation time of about 12 to 24 h, but the virus shedding started much earlier (as early as 6 hpi) than the appearance of the clinical symptoms; iii) the virus mainly targeted jejunum and ileum with a preference on the villous epithelial cells; and iv) BJ2011C spread within the gastrointestinal tract in an orderly manner; it first colonized jejunum and then spread into ileum, followed by infrequent infection of duodenum, but with no viral nucleic acids detected in situ in caecum or colon. Together, our results revealed novel information about tempo-spatial dynamics of the Chinese PEDV epidemic strain BJ2011C, which have important implication in understanding virus spread and infection.

The most shining part of this study perhaps is the application of RNAscope in situ hybridization technology to study the tissue distribution of PEDV. Traditional approach, such as antibodies-based IHC, is often limited by the lack of universally accepted standardization guidelines for antibody production. High background noise can always occur due to antigenic cross-reactivity or by alteration of binding sites of target proteins caused by tissue processing (Shi et al., 1997). Indeed, we have tried several mouse monoclonal antibodies, but they gave a

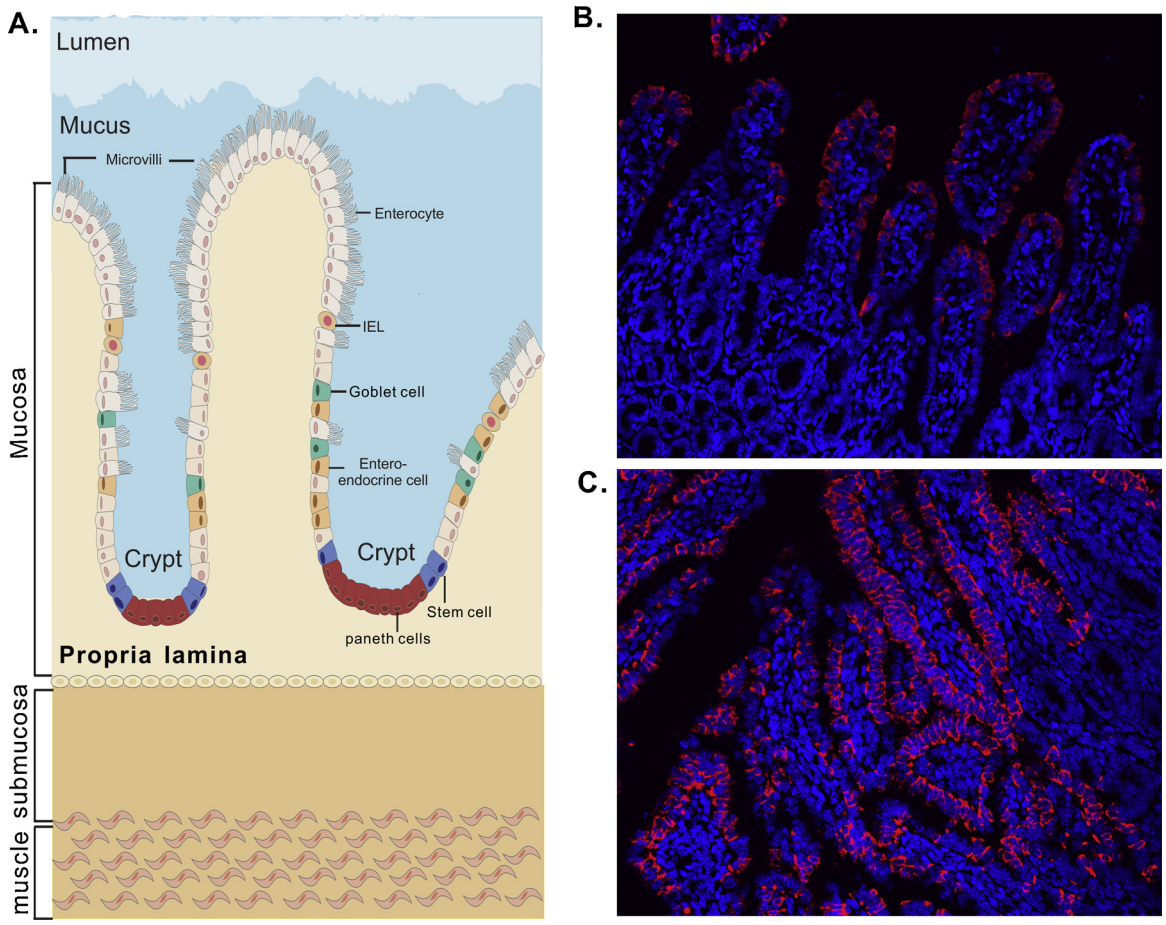

Fig. 6. PEDV BJ2011C mainly infects villous epithelial cells. (A) Diagram of Intestinal epithelial tissue. Detection of the PEDV RNA in the jejunum (B) and ileum (C) of infected piglets by ISH, showing viral RNA was mainly distributed in the villous epithelial cells. Original magnification, ×200.

high level of noise preventing from be used further (data not shown). On the other hand, despite being around for a long time, traditional in situ RNA detection techniques (ISH and FISH) generally lack robustness and sensitivity due to the limitation of probe design (Xiang and Lloyd, 2003). In contrast, RNAscope is a novel in situ RNA analysis platform for formalin-fixed, paraffin-embedded tissues that has a significantly improved signal-noise ratio (Wang et al., 2012; Zhen et al., 2013). RNAscope utilizes a unique probe design strategy in a manner of two ways (Wang et al., 2012; Zhen et al., 2013). Its signal specificity is guaranteed by the double Z probe pairs, each of which contains three parts: a region of 18–25 bp complementary to the target sequence, a spacer sequence, and a tail sequence of 14 bp. The two tails from a double Z probe pair forms a 28-base binding site for the signal pre-amplifier, but the prerequisite is that two independent probe pair (double Z probes) have to hybridize to the target sequence in tandem, thus ensuring the selective amplification of target-specific signals. The signal amplification lies in the design of the pre-amplifiers that hybridize to the 28-base binding site formed by each double Z probe. That is, each pre-amplifier contains numerous binding sites (> 20) for amplifiers that in turn contain 20 binding sites for the fluorescent labeled probe. To insure further signal amplification, ˜20 double Z target probe pairs are usually designed for each target RNA. Theoretically, it can reveal the signal of a single molecule. Since its first description around 2012, RNA Scope have been widely applied in many areas, including neuroscience, cancer biology, virology, etc (Johnson et al., 2018; Schleimann et al., 2018; Wing et al., 2018). In virology, this technique has been used to study the tissue distribution and tropism of HIV, SIV, Zika, EBV, HPV, and so on (Hsu et al., 2018; Kim et al., 2017; Marzi et al., 2018; Schleimann et al., 2018; Wang et al., 2014). And this is the first report that such an amazing technique is used on studies of PEDV. By RNAScope, we were able to reveal the dynamic nature of infection process and the tissue tropism of PEDV as described above.

Our studies revealed a difference in the results by PCR and RNAscope, as RT-PCR could detect viral nucleic acids in large intestinal sections but RNAscope failed to do so. This difference might be due to the limitation of PCR method, which detects nucleic acids at the population level. As the whole gut is a continuous channel, exfoliated small intestinal villi infected with PEDV BJ2011C would likely adhere to other parts of intestines. Once the virus replicates in the small intestines, it would be difficult to avoid the contamination. Hence, it is not surprising the large intestinal tissues are PEDV-positive by PCR. In contrast, RNAscope detects viral RNAs in situ at single cell level and can well avoid the contamination issue. Our results suggest that the inability to detect the viral RNA in situ is not a sensitivity issue but rather reflects true infection situation. For example, the PCR test revealed similar abundance of viral RNA in Jejunum and Ileum at 12 hpi (Fig S1), but we could not detect viral RNA in situ in Ileum at this time point. However, from 24 hpi, the viral RNAs in Ileum became detectable by RNAscope (Fig. 5). For large intestine, we could not detect a positive signal at any time point post infection. Thus, this observation cannot be explained simply by the sensitivity issue, but rather reflects a mode of tempo-spatial spread. The stark difference in the RNAscope signals of different tissue segments (small intestine versus large intestine) itself actually suggests a difference in the tissue preference or colonization efficiency of PEDV. In this sense, the RNAscope results provide very important insight into the infection property and dynamics of PEDV BJ2011C.

The RNAscope in situ studies revealed that BJ2011C may have

biological properties that are different from other GII strains. The first is regarding the tissue distribution of epidemic strains. Our results showed that BJ2001C was mainly in the in jejunum and ileum during infection. Interestingly, the viral nucleic acids were not detectable in situ in large intestines, although tissue damages could be discerned by H&E staining. The underlying causes are currently not clear, but we speculate that the strong diarrhea might have contributed to the damage as a mechanical stress or force. But for the PEDV strain US/Iowa/18984/2013, viral antigen in duodenum and jejunum was more than ileum at the early stage of infection in 1-day-old piglets (Madson et al., 2014). In addition, many studies using epidemic strains (e.g., PC21A, etc.) isolated in US showed that viral antigen was also detected in caecum and colon in inoculated pigs (Hou et al., 2017; Jung et al., 2015a). The difference of viral distribution may be caused by sensitivity and specificity of different detection methods, different tissue tropism among strains, difference in the duration of infection, difference in the age of the piglets, or difference in susceptibility of breed. A side-by-side comparison of different GII strains regarding their tissue distribution is clearly needed in the future.

In addition, our studies showed that PEDV BJ2011C has a short incubation period and a quick onset of clinical symptoms. The virus colonization of small intestine and the shedding could be detected at 6 hpi, a quite early stage of infection when the piglets didn't show any clinical signs. These suggest that the virus can quickly pass the harsh gastric environment and establish an efficient infection. On the other hand, for most of the epidemic strains belonging to GII such as PC21A and PC22A, the onset of clinical signs generally occurs at 1–2 days post inoculation regardless of infection dose in piglets under 7 days of age (Lin et al., 2015a, 2017). In addition, the onset of viral fecal shedding for BJ2011C was earlier than other reports using different PEDV strains. PEDV nucleic acid can be detected within 2 dpi in most studies (Fan et al., 2017; Lin et al., 2015a). Notably, since the time for the fecal sample collection in most studies was no earlier than 1 dpi, onset of viral fecal shedding may be actually earlier. In any case, the early shedding of large amount of PEDV particles prior to the clinical signs poses a significant biosecurity risk of large amount of PEDV particles prior to the clinical signs poses a significant symptom if infection is not recognized early.

5. Conclusion

By using RNAscope technology, our study revealed that the Chinese PEDV epidemic strain BJ2011C could quickly colonize gastrointestinal tract following inoculation, and spread in an orderly manner from Jejune to jejunum within infrequent and inefficient infection of duodenum. Consistent with other strains, BJ2011C mainly infects villous epithelial cells, but not crypto cells. However, BJ2011C appear to differ from other epidemic strains in tissue distribution, incubation and shedding timing, as well as the time for onset of clinical symptoms. These results highlight the differences in infection properties among PEDV GII strains, provide useful information for further studies on the mechanisms underlying the viral pathogenesis of PEDV in neonatal piglets, and have implications in the PED control.

Funding

This work was supported by National Key Research and Development Program (2016YFD0500101) (http://program.most.gov.cn/) from the Ministry of Science and Technology of China, the China National Thousand Youth Talents program (1051-21986001), and the earmarked fund for China Agriculture Research System (CARS-35) from the Chinese Ministry of Agriculture.

Appendix A. Supplementary data

Supplementary material related to this article can be found, in the online version, at doi:https://doi.org/10.1016/j.vetmic.2019.07.003.

References

Al, W.L.E., 2012. New variants of Porcine Epidemic Diarrhea Virus, China, 2011 - volume 18, number 8—august 2012 - emerging infectious disease journal - CDC. Emerging Infect. Dis. 18, 1350–1353.
Amimo, J.O., Vlasova, A.N., Saif, L.J., 2013a. Detection and genetic diversity of porcine group A rotaviruses in historic (2004) and recent (2011 and 2012) swine fecal samples in Ohio: predominance of the G9P[13] genotype in nursing piglets. J. Clin. Microbiol. 51, 1142–1151.
Amimo, J.O., Vlasova, A.N., Saif, L.J., 2013b. Prevalence and genetic heterogeneity of porcine group C rotaviruses in nursing and weaned piglets in Ohio, USA and identification of a potential new VP4 genotype. Vet. Microbiol. 164, 27–38.
Changhee, L., 2015. Porcine epidemic diarrhea virus: an emerging and re-emerging epizootic swine virus. Virol. J. 12, 1–16.
Choudhury, B., Dastjerdi, A., Doyle, N., Frossard, J.P., Steinbach, F., 2016. From the field to the lab-an European view on the global spread of PEDV. Virus Res. 226, 40–49.
Elena, T.O.M., Rolando, B.F., Mireya, J.R., Alicia, S.G., Hernández-Villegas, E.N., Becerra-Hernández, J.F., Elena, S.S.R., 2016. Isolation and characterization of porcine epidemic diarrhea virus associated with the 2014 disease outbreak in Mexico: case report. BMC Vet. Res. 12, 132.
Fan, B., Yu, Z., Pang, F., Xu, X., Zhang, B., Guo, R., He, K., Li, B., 2017. Characterization of a pathogenic full-length cDNA clone of a virulent porcine epidemic diarrhea virus strain AH2012/12 in China. Virology 500, 50–61.
Hofmann, M., Wyler, R., 1988. Propagation of the virus of porcine epidemic diarrhea in cell culture. J. Clin. Microbiol. 26, 2235–2239.
Hou, Y., Lin, C.M., Yokoyama, M., Yount, B.L., Marthaler, D., Douglas, A.L., Ghimire, S., Qin, Y., Baric, R.S., Saif, L.J., 2017. Deletion of a 197-Amino-Acid region in the N-Terminal domain of spike protein attenuates porcine epidemic diarrhea virus in piglets. J. Virol. 91 JVI. 00227-00217.
Hsu, D.C., Sunyakumthorn, P., Wegner, M., Schuetz, A., Silsorn, D., Estes, J.D., Deleage, C., Tomusange, K., Lakhashe, S.K., Ruprecht, R.M., 2018. Central nervous system inflammation and infection during early, non-accelerated simian-human immunodeficiency virus infection in Rhesus macaques. J. Virol. 92 JVI.00222-00218.
C.K.B.K.T.J.Y.K.D. Hur, 1993. Isolation of porcine epidemic diarrhea virus (PEDV) in Korea. Korean J. Vet. Res. 33, 249–254.
Jensen, E., 2014. Technical review: in situ hybridization. Anat. Rec. 297, 1349–1353.
Johnson, M.B., Sun, X., Kodani, A., Borgesmonroy, R., Girskis, K.M., Ryu, S.C., Wang, P.P., Patel, K., Gonzalez, D.M., Woo, Y.M., 2018. Aspm knockout ferret reveals an evolutionary mechanism governing cerebral cortical size. Nature 556, 370–375.
Jung, K., Annamalai, T., Lu, Z., Saif, L.J., 2015a. Comparative pathogenesis of US porcine epidemic diarrhea virus (PEDV) strain PC21A in conventional 9-day-old nursing piglets vs. 26-day-old weaned pigs. Vet. Microbiol. 178, 31–40.
Jung, K., Hu, H., Eyerly, B., Lu, Z., Chepngeno, J., Saif, L.J., 2015b. Pathogenicity of 2 porcine deltacoronavirus strains in gnotobiotic pigs. Emerg. Infect. Dis. 21, 650–654.
Jung, K., Wang, Q., Scheuer, K.A., Lu, Z., Zhang, Y., Saif, L.J., 2014. Pathology of US porcine epidemic diarrhea virus strain PC21A in gnotobiotic pigs. Emerg. Infect. Dis. 20, 662–665.
Kim, L., Chang, K.-O., Sestak, K., Parwani, A., Saif, L.J., 2000. Development of a reverse transcription-nested polymerase chain reaction assay for differential diagnosis of transmissible gastroenteritis virus and porcine respiratory coronavirus from feces and nasal swabs of infected pigs. J. Vet. Diagn. Invest. 12, 385–388.
Kim, Y., Kim, H.S., Park, J.S., Kim, C.J., Kim, W.H., 2017. Identification of epstein-barr virus in the human placenta and its pathologic characteristics. J. Korean Med. Sci. 32, 1959–1966.
Li, J., Jin, Z., Gao, Y., Zhou, L., Ge, X., Guo, X., Han, J., Yang, H., 2017. Development of the full-length cDNA clones of two porcine epidemic diarrhea disease virus isolates with different virulence. PLoS One 12, e0173998.
Lin, C.M., Annamalai, T., Liu, X., Gao, X., Lu, Z., El-Tholoth, M., Hu, H., Saif, L.J., Wang, Q., 2015a. Experimental infection of a US spike-insertion deletion porcine epidemic diarrhea virus in conventional nursing piglets and cross-protection to the original US PEDV infection. Vet. Res. 46, 134.
Lin, C.M., Annamalai, T., Liu, X., Gao, X., Lu, Z., Eltholoth, M., Hu, H., Saif, L.J., Wang, Q., 2015b. Experimental infection of a US spike-insertion deletion porcine epidemic diarrhea virus in conventional nursing piglets and cross-protection to the original US PEDV infection. Vet. Res. 46, 134.
Lin, C.M., Hou, Y., Marthaler, D.G., Gao, X., Liu, X., Zheng, L., Saif, L.J., Wang, Q., 2017. Attenuation of an original US porcine epidemic diarrhea virus strain PC22A via serial cell culture passage. Vet. Microbiol. 201, 62–71.
Madson, D.M., Magstadt, D.R., Arruda, P.H.E., Hoang, H., Sun, D., Bower, L.P., Bhandari, M., Burrough, E.R., Gauger, P.C., Pillatzki, A.E., 2014. Pathogenesis of porcine epidemic diarrhea virus isolate (US/Iowa/18984/2013) in 3-week-old weaned pigs. Vet. Microbiol. 174, 60–68.
Marzi, A., Emanuel, J., Callison, J., Mcnally, K.L., Arndt, N., Chadinha, S., Martellaro, C., Rosenke, R., Scott, D.P., Safronetz, D., 2018. Lethal zika virus disease models in young and older interferon α/β receptor knock out mice. Front. Cell. Infect. Microbiol. 8, 117.
Min, S., Jiale, M., Yanan, W., Ming, W., Wenchao, S., Wei, Z., Chengping, L., Huochun, Y., 2015. Genomic and epidemiological characteristics provide new insights into the phylogeographical and spatiotemporal spread of porcine epidemic diarrhea virus in Asia. J. Clin. Microbiol. 53, 1484–1492.
Pensaert, M.B., Debouck, 1978. A new coronavirus-like particle associated with diarrhea in swine. Arch. Virol. 58, 243–247.
Rui-Qin, S., Ru-Jian, C., Ya-Qiang, C., Peng-Shuai, L., De-Kun, C., Chang-Xu, S., 2012.

Outbreak of porcine epidemic diarrhea in suckling piglets, China. Emerg. Infect. Dis. 18, 161–163.
Schleimann, M.H., Leth, S., Krarup, A.R., Mortensen, J., Barstad, B., Zaccarin, M., Denton, P.W., Mohey, R., 2018. Acute appendicitis as the initial clinical presentation of primary HIV-1 infection. Open Forum Infect. Dis. 5.
Shi, S.R., Cote, R.J., Young, L., Taylor, C.R., 1997. Antigen retrieval immunohistochemistry: practice and development. J. Histotechnol. 20, 145–154.
Shibata, I., Tsuda, T., Mori, M., Ono, M., Sueyoshi, M., Uruno, K., 2000. Isolation of porcine epidemic diarrhea virus in porcine cell cultures and experimental infection of pigs of different ages. Vet. Microbiol. 72, 173–182.
Song, D., Park, B., 2012. Porcine epidemic diarrhoea virus: a comprehensive review of molecular epidemiology, diagnosis, and vaccines. Virus Genes 44, 167–175.
Stevenson, G.W., Hoang, H., Schwartz, K.J., Burrough, E.R., Sun, D., Madson, D., Cooper, V.L., Pillatzki, A., Gauger, P., Schmitt, B.J., 2013a. Emergence of Porcine epidemic diarrhea virus in the United States: clinical signs, lesions, and viral genomic sequences. J. Vet. Diagn. Invest. 25, 649.
Stevenson, G.W., Hoang, H., Schwartz, K.J., Burrough, E.R., Sun, D., Madson, D.M., Cooper, V.L., Pillatzki, A.E., Gauger, P.C., Schmitt, B.J., 2013b. Emergence of Porcine epidemic diarrhea virus in the United States: clinical signs, lesions, and viral genomic sequences. J. Vet. Diagn. Invest. 25, 649–654.
Sueyoshi, M., Tsuda, T., Yamazaki, K., Yoshida, K., Nakazawa, M., Sato, K., Minami, T., Iwashita, K., Watanabe, M., Suzuki, Y., 1995. An immunohistochemical investigation of porcine epidemic diarrhoea. J. Comp. Pathol. 113, 59–67.
Sun, M., Ma, J., Wang, Y., Wang, M., Song, W., Zhang, W., Lu, C., Yao, H., 2015. Genomic and epidemiological characteristics provide new insights into the phylogeographical and spatiotemporal spread of porcine epidemic diarrhea virus in Asia. J. Clin. Microbiol. 53, 1484–1492.
Sun, R.Q., Cai, R.J., Chen, Y.Q., Liang, P.S., Chen, D.K., Song, C.X., 2012. Outbreak of porcine epidemic diarrhea in suckling piglets, China. Emerg. Infect. Dis. 18, 161–163.
Takahashi, K., Okada, K., Ohshima, K., 1983. An outbreak of swine diarrhea of a new-type associated with coronavirus-like particles in Japan. Nihon Juigaku Zasshi Japanese J. Vet. Sci. 45, 829.
Vlasova, A.N., Marthaler, D., Wang, Q., Culhane, M.R., Rossow, K.D., Rovira, A., Collins, J., Saif, L.J., 2014. Distinct characteristics and complex evolution of PEDV strains, North America, may 2013–February 2014. Emerg. Infect. Dis. 20, 1620.
Wang, D., Fang, L., Xiao, S., 2016. Porcine epidemic diarrhea in China. Virus Res. 226, 7–13.
Wang, D., Ge, X., Chen, D., Li, J., Cai, Y., Deng, J., Zhou, L., Guo, X., Han, J., Yang, H., 2018. The S gene is necessary but not sufficient for the virulence of porcine epidemic diarrhea virus novel variant strain BJ2011C. J. Virol. 92.
Wang, F., Flanagan, J., Su, N., Wang, L.C., Bui, S., Nielson, A., Wu, X., Vo, H.T., Ma, X.J., Luo, Y., 2012. RNAscope: a novel in situ RNA analysis platform for formalin-fixed, paraffin-embedded tissues. J. Mol. Diagn. 14, 22–29.
Wang, H., Wang, M.X., Su, N., Wang, L.C., Wu, X., Bui, S., Nielsen, A., Vo, H.T., Nguyen, N., Luo, Y., 2014. RNAscope for in situ detection of transcriptionally active human papillomavirus in head and neck squamous cell carcinoma. J. Vis. Exp. 85 e51426-e51426.
Wing, A., Fajardo, C.A., Posey, A.D., Shaw, C.E., Da, T., Young, R.M., Alemany, R., June, C.H., Guedan, S., 2018. Improving CART-Cell therapy of solid tumors with oncolytic virus–Driven production of a bispecific T-cell engager. Cancer Immunol. Res. 6, 605–616.
Xiang, Q., Lloyd, R.V., 2003. Recent developments in signal amplification methods for in situ hybridization. Diagn. Mol. Pathol. 12, 1–13.
Xiao-Meng, W., Bei-Bei, N., He, Y., Dong-Sheng, G., Xia, Y., Lu, C., Hong-Tao, C., Jun, Z., Chuan-Qing, W., 2013. Genetic properties of endemic Chinese porcine epidemic diarrhea virus strains isolated since 2010. Arch. Virol. 158, 2487–2494.
Zhen, W., Portier, B.P., Gruver, A.M., Son, B., Hongwei, W., Nan, S., Hong-Thuy, V., Xiao-Jun, M., Yuling, L., G Thomas, B., 2013. Automated quantitative RNA in situ hybridization for resolution of equivocal and heterogeneous ERBB2 (HER2) status in invasive breast carcinoma. J. Mol. Diagn. 15, 210–219.